

Shrink fit tool holder connection stiffness/damping modeling for frequency response prediction in milling, Part 1: Receptance model

*Tony L. Schmitz, Kevin Powell, Dongki Won, G. Scott Duncan, W. Gregory Sawyer,
John C. Ziegert*

*Department of Mechanical and Aerospace Engineering, University of Florida,
Gainesville, FL 32611, tschmitz@ufl.edu*

Abstract: We present a finite element modeling approach to determine the stiffness and damping behavior between the tool and holder in thermal shrink fit connections. The continuous contact stiffness/damping profile between the holder and portion of the tool inside the holder is approximated by defining coordinates along the contact length interface and assigning position-dependent stiffness and equivalent viscous damping values between the tool and holder. These values are incorporated into the third generation Receptance Coupling Substructure Analysis (RCSA) method, which is used to predict the tool point frequency response for milling applications. Once the holder and inserted tool section are connected using the finite element analysis-based stiffness and damping values, this subassembly is then rigidly coupled to the (measured) spindle-holder base and (modeled) tool. The receptance coupling model is presented here in Part 1 of the paper. The finite element model is described in Part 2. Experimental validation is also provided.

Keywords: receptance, high-speed machining, finite element

1. INTRODUCTION

Discrete part production by milling remains an important manufacturing capability. However, there are many potential obstacles to producing quality parts at low cost in a timely manner. One particular limitation that has received considerable attention in the literature is chatter, or unstable machining; a second is surface location error, or an error in the part dimension caused by dynamic deflections of the tool (and potentially the part/fixture) during stable cutting. In both cases, a primary factor affecting the process performance is the system frequency response function, or FRF.

The system FRF, often dominated by the flexibility of the tool-holder-spindle assembly as reflected at the tool's free end, can be obtained using impact testing, where an instrumented hammer is used to excite the tool at its free end (i.e., the tool point) and the resulting vibration is measured using an appropriate transducer, typically a low mass accelerometer. However, due to the large number of spindle, holder, and tool combinations that may be available in a particular production facility, the required

testing time can be significant. Further, the measured response is often strongly dependent on the tool overhang length. Therefore, a model which is able to predict the tool point response based on minimum input data is the preferred alternative [Schmitz *et al.*, 2000, 2001a, 2001b, 2003, 2005a, 2005b; Burns *et al.*, 2005; Cheng *et al.*, 2005; Yigit *et al.*, 2002; Park *et al.*, 2003; Kivanc *et al.*, 2004; Agapiou, 2004; Zhang *et al.*, 2003].

The purpose of this paper is to build on the previous work of Schmitz *et al.* [Schmitz *et al.*, 2000, 2001a, 2001b, 2003, 2005a, 2005b; Burns *et al.*, 2005; Cheng *et al.*, 2005], which describes tool point FRF, or receptance, prediction using the Receptance Coupling Substructure Analysis (RCSA) method. In these previous studies, two and three component models of the machine-spindle-holder-tool assembly were defined. In the two component model, the machine-spindle-holder displacement-to-force receptance was recorded at the free end of the holder using impact testing, while the tool was modeled analytically. The tool and machine-spindle-holder substructure receptances were then coupled through translational and rotational springs and dampers, where their values were determined through a nonlinear least squares fitting procedure. In this initial work the displacement-to-moment, rotation-to-force, and rotation-to-moment receptances at the free end of the holder were assumed zero (i.e., perfectly rigid).

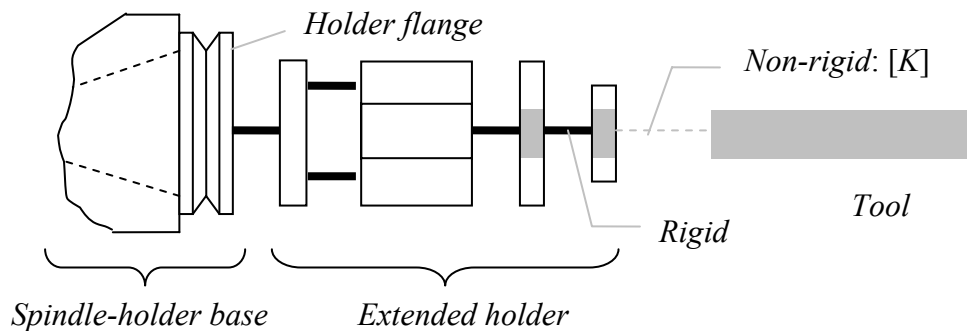


Figure 1; Second generation RCSA model – the finite tool-holder stiffness/damping was represented by the empirical stiffness matrix, K , which was used to couple the overhung portion of the tool to the rest of the assembly. All other connections were rigid.

In the second generation three component model, the machine-spindle-holder substructure was separated into two parts: 1) the machine, spindle, holder taper, and holder flange (or spindle-holder base subassembly); and 2) the remaining portion of the holder from the flange to the free end (the extended holder subassembly). The rotation-to-force/moment and displacement-to-moment receptances for the free end of the spindle-holder base subassembly were determined using displacement-to-force measurements and finite difference computations. The experimental procedure involved recording direct and cross displacement-to-force measurements of a simple geometry ‘standard’ holder clamped in the spindle and calculating the receptances at the free end of the assembly by finite differences [Schmitz *et al.*, 2005a, 2005b]. The portion of the

standard holder beyond the flange was then removed in simulation using an inverse receptance coupling approach to identify the four spindle-holder base subassembly receptances (i.e., displacement/rotation-to-force/moment). These receptances were then coupled to models of the actual holder and tool. Again, to account for finite stiffness and energy dissipation (i.e., damping) in the tool-holder connection, the tool was coupled to the holder using translational and rotational springs and dampers, assembled in the matrix K (Eq. 1), where k_{yf} is the displacement-to-force stiffness, $k_{\theta m}$ is the rotation-to-moment stiffness, c_{yf} and $c_{\theta m}$ are the corresponding viscous damping terms, and ω is the circular frequency (rad/s). See Fig. 1. The portion of the holder with the tool inserted was treated using a composite modulus and mass in the event that the holder and tool materials were different, such as a steel holder and carbide tool.

$$K = \begin{bmatrix} k_{yf} + i\omega \cdot c_{yf} & 0 \\ 0 & k_{\theta m} + i\omega \cdot c_{\theta m} \end{bmatrix} \quad (1)$$

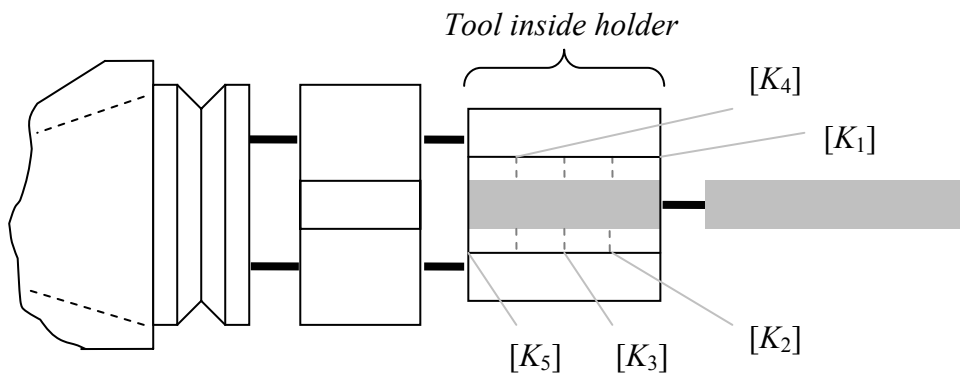


Figure 2; Third generation RCSA model – the finite stiffness/damping between the tool and holder is represented by multiple K matrices determined from finite element simulation.

In this work, we extend the three component model to include multiple connections between the tool and holder along the interference contact within the holder (rather than at the end of the holder as before). This is shown schematically in Fig. 2, where multiple complex stiffness matrices, K_i , describe the connection parameters at each location. We believe this to be a preferred solution because the stiffness/damping is now located at the appropriate locations, rather than artificially at the junction between the portions of the tool inside and outside the holder. We note, however, that the coordinate-based stiffness/damping analysis is an approximation of the continuous contact stiffness/damping profile between the holder and portion of the tool inside the holder.

In this new model the fully populated K matrix is defined as shown in Eq. 2, which now accounts for the displacement imposed by moment and the rotation caused by force through the non-zero off diagonal terms. Finite element models are developed in Part 2 of this paper to determine the position-dependent stiffness and equivalent viscous

damping values for a thermal shrink fit connection between the tool and holder, which represents the preferred interface for high-speed milling applications. Using these values, the tool point FRF is predicted *a priori* and compared to measurements for a number of cases. No fitting parameters are applied in this analysis.

$$K = \begin{bmatrix} k_{yf} + i\omega \cdot c_{yf} & k_{ym} + i\omega \cdot c_{ym} \\ k_{\theta f} + i\omega \cdot c_{\theta f} & k_{\theta m} + i\omega \cdot c_{\theta m} \end{bmatrix} \quad (2)$$

The paper is organized as follows. First, the RCSA approach for joining the portions of the tool and holder which comprise the shrink fit connection is described. Second, the RCSA equation for the entire tool-holder-spindle assembly is provided. Finally, conclusions are presented.

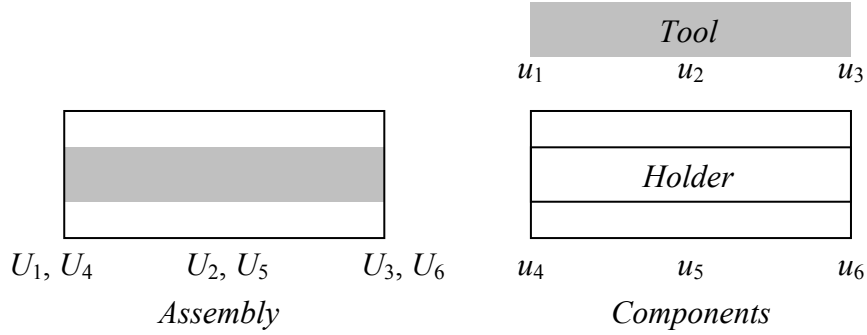


Figure 3; Tool-in-holder assembly and components.

2. MULTIPLE POINT COUPLING FOR THE TOOL-HOLDER CONNECTION

To demonstrate the coupling between the concentric inner tool and outer holder components, the case of $n = 3$ connection coordinates, located at the ends of the contact length and at the mid-point, is now presented. The portions of the tool and holder in shrink fit contact are treated as free-free beams. For $n = 3$, a total of six component coordinates is obtained – three each on the internal tool and external holder (see Fig. 3) [Schmitz *et al.*, 2006]. The component (i.e., tool and holder) displacement/rotations can be written as:

$$\begin{aligned} u_1 &= R_{11}q_1 + R_{12}q_2 + R_{13}q_3 & u_2 &= R_{21}q_1 + R_{22}q_2 + R_{23}q_3 \\ u_3 &= R_{31}q_1 + R_{32}q_2 + R_{33}q_3 & u_4 &= R_{44}q_4 + R_{45}q_5 + R_{46}q_6 \\ u_5 &= R_{54}q_4 + R_{55}q_5 + R_{56}q_6 & u_6 &= R_{64}q_4 + R_{65}q_5 + R_{66}q_6, \end{aligned} \quad (3)$$

where a matrix formalism has been adopted [Park *et al.*, 2003]. Here, $u_i = \{y_i \ \theta_i\}^T$ are the component displacements/rotations; $q_i = \{f_i \ m_i\}^T$ are the component

forces/moments; and $R_{ij}(\omega) = \begin{bmatrix} \frac{y_i}{f_j} & \frac{y_i}{m_j} \\ \frac{\theta_i}{f_j} & \frac{\theta_i}{m_j} \end{bmatrix} = \begin{bmatrix} h_{ij} & l_{ij} \\ n_{ij} & p_{ij} \end{bmatrix}$ are the component receptances.

The compatibility conditions for the flexible/damped shrink fit connection are:

$$K_1(u_4 - u_1) = -q_4, \quad K_2(u_5 - u_2) = -q_5, \quad \text{and} \quad K_3(u_6 - u_3) = -q_6, \quad (4)$$

where K_i is given by Eq. 2 and the component and assembly coordinates are defined at the same spatial locations so that $u_i = U_i$, $i = 1$ to 6. If the assembly direct response at the left end, $G_{11}(\omega)$, is to be determined, Q_1 is applied to coordinate U_1 of the assembly (the upper case variables denote assembly coordinates, forces, and moments). The equilibrium conditions are then:

$$q_1 + q_4 = Q_1, \quad q_2 + q_5 = 0, \quad \text{and} \quad q_3 + q_6 = 0. \quad (5)$$

G_{11} is determined in steps using the relevant equations. The first step is to insert the component displacement/rotation expressions into the compatibility conditions as shown in Eq. 6.

$$\begin{aligned} R_{11}q_1 + R_{12}q_2 + R_{13}q_3 &= R_{44}q_4 + R_{45}q_5 + R_{46}q_6 + K_1^{-1}q_4 \\ R_{21}q_1 + R_{22}q_2 + R_{23}q_3 &= R_{54}q_4 + R_{55}q_5 + R_{56}q_6 + K_2^{-1}q_5 \\ R_{31}q_1 + R_{32}q_2 + R_{33}q_3 &= R_{64}q_4 + R_{65}q_5 + R_{66}q_6 + K_3^{-1}q_6 \end{aligned} \quad (6)$$

The next step is to substitute $q_4 = Q_1 - q_1$, $q_5 = -q_2$, and $q_6 = -q_3$ and rearrange to obtain:

$$\begin{bmatrix} R_{11} + R_{44} + K_1^{-1} & R_{12} + R_{45} & R_{13} + R_{46} \\ R_{21} + R_{54} & R_{22} + R_{55} + K_2^{-1} & R_{23} + R_{56} \\ R_{31} + R_{64} & R_{32} + R_{65} & R_{33} + R_{66} + K_3^{-1} \end{bmatrix} \begin{Bmatrix} q_1 \\ q_2 \\ q_3 \end{Bmatrix} = Q_1 \begin{bmatrix} R_{44} + K_1^{-1} \\ R_{54} \\ R_{64} \end{bmatrix}, \quad (7)$$

which gives the relationship between the component forces/moments and externally applied force/moment in matrix form. For this example, G_{11} can be expressed as:

$$G_{11} = \frac{U_1}{Q_1} = \frac{u_1}{Q_1} = R_{11} \frac{q_1}{Q_1} + R_{12} \frac{q_2}{Q_1} + R_{13} \frac{q_3}{Q_1}, \quad (8)$$

so the ratios $\frac{q_1}{Q_1}$, $\frac{q_2}{Q_1}$, and $\frac{q_3}{Q_1}$ are required. These can be determined by rearranging Eq. 7:

$$\frac{1}{Q_1} \begin{Bmatrix} q_1 \\ q_2 \\ q_3 \end{Bmatrix} = \begin{bmatrix} R_{11} + R_{44} + K_1^{-1} & R_{12} + R_{45} & R_{13} + R_{46} \\ R_{21} + R_{54} & R_{22} + R_{55} + K_2^{-1} & R_{23} + R_{54} \\ R_{31} + R_{64} & R_{32} + R_{65} & R_{33} + R_{66} + K_3^{-1} \end{bmatrix}^{-1} \begin{bmatrix} R_{44} + K_1^{-1} \\ R_{54} \\ R_{64} \end{bmatrix} = [A],$$

where $[A]$ is a 6 by 2, or $2n$ by 2, by N matrix (N is the number of points in the frequency vector, ω). The reader may note that the matrix size is 6 by 2 because R_{ij} is a 2 by 2 matrix. The matrix A is partitioned as follows: the first two rows of A give $\frac{q_1}{Q_1}$;

the second two rows provide $\frac{q_2}{Q_1}$; and the final two rows give $\frac{q_3}{Q_1}$. The desired direct receptances can then be computed from Eq. 8.

This 3-point coupling example can be extended to n coupling points by recognizing the recursive pattern in $[A]$. If the same coordinate numbering scheme is observed (i.e., coordinates 1 to n on the tool and $n+1$ to $2n$ on the holder), $[A]$ is given by:

$$[A] = \begin{bmatrix} R_{11} + R_{n+1,n+1} + K_1^{-1} & R_{12} + R_{n+1,n+2} & \cdots & R_{1n} + R_{n+1,2n} \\ R_{21} + R_{n+2,n+1} & R_{22} + R_{n+2,n+2} + K_2^{-1} & \cdots & R_{2n} + R_{n+2,2n} \\ \vdots & \vdots & \ddots & \vdots \\ R_{n1} + R_{2n,n+1} & R_{n2} + R_{2n,n+2} & \cdots & R_{nn} + R_{2n,2n} + K_n^{-1} \end{bmatrix}^{-1} \begin{bmatrix} R_{n+1,n+1} + K_1^{-1} \\ R_{n+2,n+1} \\ \vdots \\ R_{2n,n+1} \end{bmatrix}.$$

This matrix can again be partitioned to find $\frac{q_1}{Q_1}$, $\frac{q_2}{Q_1}$, ..., $\frac{q_n}{Q_1}$. The assembly

receptances G_{11} can then be found using $G_{11} = R_{11} \frac{q_1}{Q_1} + R_{12} \frac{q_2}{Q_1} + \cdots + R_{1n} \frac{q_n}{Q_1}$. The

following sections detail the development of the required receptances, R_{ij} , for the inner tool and outer holder.

2.1. Inner tool receptances

The inner tool receptance matrix is composed of n^2 R_{ij} terms ($i = 1$ to n and $j = 1$ to n).

However, by observing reciprocity (i.e., R_{ii} is symmetric and $R_{ji} = \begin{bmatrix} h_{ij} & n_{ij} \\ l_{ij} & p_{ij} \end{bmatrix}$), it is

only necessary to determine the upper triangular portion of the square R_{ij} matrix, or $\sum_{i=1}^n i$ terms. The corners of the upper triangular portion of the matrix, R_{11} , R_{1n} , and R_{nn} , may be found using the closed-form receptances for uniform Euler-Bernoulli beams developed by Bishop and Johnson [Bishop *et al.*, 1960] directly, where the full beam length, L , is used in these computations¹. The remaining terms in the first row of the R_{ij} matrix, R_{12} , R_{13} , \dots , $R_{1,n-1}$ are determined next. To find R_{12} , q_2 is applied at coordinate u_2 as shown in Fig. 4.

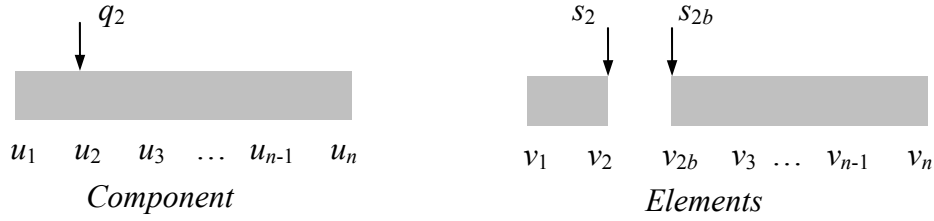


Figure 4; Inner tool R_{12} determination.

The cylinder component must now be sectioned at coordinate u_2 into two elements with generalized receptance matrices E_{ij} and coordinates v_1 to v_n (see Fig. 4). For equally-spaced connection coordinates, the length of the left element is $\Delta L = \frac{L}{n-1}$, while the right element length is $L - \Delta L$. The element displacements/rotations can be written as:

$$v_1 = E_{12}s_2, \quad v_2 = E_{22}s_2, \quad \text{and} \quad v_{2b} = E_{2b2b}s_{2b}, \quad (9)$$

where s_1 , s_2 , and s_{2b} are the nonzero element forces. The compatibility conditions for the rigid coupling between elements are given in Eq. 10. The associated equilibrium condition is provided in Eq. 11.

$$v_2 - v_{2b} = 0 \quad \text{and} \quad v_i = V_i, \quad i = 1 \text{ to } n \quad (10)$$

$$s_2 + s_{2b} = q_2 \quad (11)$$

Similar to the previous results, substitution of the element displacement/rotations and equilibrium condition into the compatibility conditions yields the following expression for R_{12} :

$$R_{12} = E_{12} \left(E_{22} + E_{2b2b} \right)^{-1} E_{2b2b}. \quad (12)$$

¹ Alternately, Timoshenko beam receptances can be applied.

To find R_{13} , q_3 is applied at u_3 . The required left and right elements now have the lengths $2\Delta L$ and $L-2\Delta L$, respectively. The equation for R_{13} is:

$$R_{13} = E_{13} (E_{33} + E_{3b3b})^{-1} E_{3b3b}. \quad (13)$$

The recursive pattern is immediately apparent so that R_{1j} is defined by:

$$R_{1j} = E_{1j} (E_{jj} + E_{jbjb})^{-1} E_{jbjb}, \text{ where } j = 2 \text{ to } n-1 \text{ is the column number.} \quad (14)$$

Also, E_{1j} describes the cross receptances for the left element (with a length of $(j-1)\Delta L$), E_{ij} provides the direct receptances at the right end of the left element, and E_{jbjb} gives the direct receptances at the left end of the right element (with a length of $L-(j-1)\Delta L$).

The n^{th} column of the R_{ij} matrix is defined next. In this case, q_n is applied to the coordinate u_n at the right end of the cylinder component in order to find R_{in} , where $i = 2$ to $n-1$ is the row number. The recursive form is:

$$R_{in} = E_{ii} (E_{ii} + E_{ibib})^{-1} E_{ibn}, \quad (15)$$

where E_{ii} and E_{ibib} are defined in the same way as E_{jj} and E_{jbjb} , respectively. The E_{ibn} cross receptances for the right element are calculated using an element length of $L-(i-1)\Delta L$.

The next terms to describe are the on-diagonal receptances R_{ii} , $i = 2$ to $n-1$. These can be written as:

$$R_{ii} = E_{ii} (E_{ii} + E_{ibib})^{-1} E_{ibib}. \quad (16)$$

Again, E_{ii} , the direct receptances at the right end of the left element and E_{ibib} , the direct receptances at the left end of the right element, have the same definitions as previously provided.

The remaining receptances are those R_{ij} terms above the on-diagonal, exclusive of the 1st row and n^{th} column. These receptances are determined column-by-column. For a particular column, $j = 2$ to $n-1$, R_{ij} is given by:

$$R_{ij} = E_{ij} (E_{jj} + E_{jbjb})^{-1} E_{jbjb}, \quad i = 2 \text{ to } j-1. \quad (17)$$

In this equation, the left element (with direct receptances E_{jj}) has a length of $(j-1)\Delta L$ and the right element (with direct receptances E_{jbjb}) has a length of $L-(j-1)\Delta L$. However, the E_{ij} element receptances cannot be determined directly from the Bishop and Johnson formulation [Bishop *et al.*, 1960]. In this case, subelement receptances S_{ij} must be defined. This is demonstrated by solving for R_{23} .

To find R_{23} , q_3 is applied to coordinate u_2 . The cylinder component is then split at coordinate u_3 to define two elements (see Fig. 5). The element displacements/rotations are given by:

$$v_2 = E_{23}s_3, \quad v_3 = E_{33}s_3, \quad \text{and} \quad v_{3b} = E_{3b3b}s_{3b}. \quad (18)$$

The rigid connection compatibility conditions are shown in Eq. 19 and the equilibrium condition in Eq. 20.

$$v_3 - v_{3b} = 0 \quad \text{and} \quad v_i = u_i, \quad i = 1 \text{ to } n. \quad (19)$$

$$s_3 + s_{3b} = q_3. \quad (20)$$

Using these equations, it is found that:

$$R_{23} = E_{23}(E_{33} + E_{3b3b})^{-1}E_{3b23}. \quad (21)$$

As noted, E_{23} , the cross receptances at coordinate v_2 of the left element due to the application of s_3 at coordinate v_3 , is determined by separating the left element (with a length of $(j-1)\Delta L$), into two subelements at coordinate v_2 (see Fig. 5). The length of the left subelement is $(i-1)\Delta L = (2-1)\Delta L = \Delta L$, while the length of the right subelement is $(j-i)\Delta L = (3-2)\Delta L = \Delta L$.

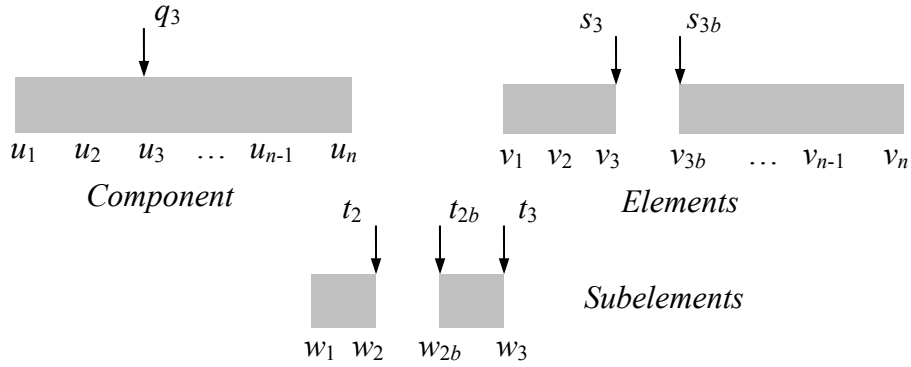


Figure 5; Inner tool R_{23} determination.

Using the displacement/rotation, compatibility, and equilibrium equations, it is found that:

$$E_{23} = S_{22}(S_{22} + S_{2b2b})^{-1}S_{2b3}, \quad (22)$$

where S_{22} gives the direct receptances at the right end of the left subelement, S_{2b2b} contains the direct receptances at the left end of the right subelement, and S_{2b3}

represents the cross receptances for the right subelement. The recursive formulation for this equation is:

$$E_{ij} = S_{ii} (S_{ii} + S_{ibib})^{-1} S_{ibj}, \quad i = 2 \text{ to } j-1 \text{ and } j = 2 \text{ to } n-1. \quad (23)$$

All terms in the upper triangular portion of the R_{ij} matrix for the inner cylinder have now been determined. The lower triangular portion, excluding the on-diagonal terms, is found by observing the symmetry rules given previously as demonstrated by the following pseudo-code.

```

for  $i = 1$  to  $n-1$ 
  for  $j = i+1$  to  $n$ 
     $R_{ji} = \begin{bmatrix} h_{ij} & n_{ij} \\ l_{ij} & p_{ij} \end{bmatrix}$ 
  next  $j$ 
next  $i$ 

```

2.2. Outer holder receptances

To find the R_{ij} matrix for the outer holder, n is added to each coordinate number (i.e., the coordinate number for the tube left end is $n+1$ and the right end coordinate number is $2n$) and the beam geometry and material properties are updated for the receptance computations. All other definitions remain the same.

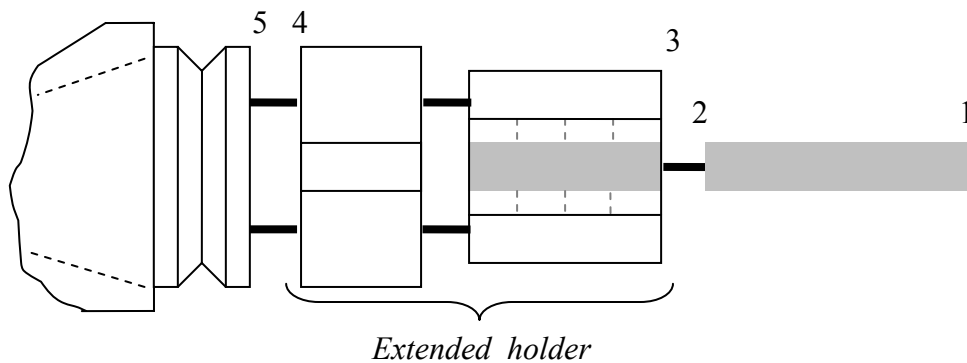


Figure 6; Third generation RCSA model – coordinate definitions.

3. TOOL-HOLDER-SPINDLE ASSEMBLY RCSA EQUATION

Once the shrink fit connection stiffness is incorporated into the tool-holder assembly (for the portion of the tool inside the holder) as defined in Section 2, the remaining components can be rigidly coupled. Assembly coordinate definitions for the overhung portion of the tool (1-2), extended holder (3-4), and spindle-holder base (5) are shown

in Fig. 6. The corresponding RCSA equation for the assembly receptances at the tool point is obtained by: 1) rigidly coupling the overhung free-free tool to the free-free tool-extended holder to determine the new subassembly direct receptances at each end, GS_{11} and GS_{44} , and the cross receptances, GS_{14} and GS_{41} ; and 2) using the standard holder and finite difference calculations to determine the four receptances at the free end of the standard holder (mounted in the spindle in question), removing the portion of the standard holder beyond the flange using inverse RCSA, and defining the direct receptance at the free end of the spindle-holder base subassembly, GS_{55} . See Eq. 24, where $H_{11}(\omega) = \frac{Y_1}{F_1}$ is the frequency response generally required for milling stability and surface location error analyses. Additional details are available in [Schmitz *et al.* 2005a, 2005b].

$$G_{11} = \begin{bmatrix} H_{11} & L_{11} \\ N_{11} & P_{11} \end{bmatrix} = GS_{11} - GS_{14}(GS_{44} + GS_{55})^{-1}GS_{41} \quad (24)$$

4. CONCLUSIONS

This paper describes the third generation Receptance Coupling Substructure Analysis (RCSA) model for tool point frequency response prediction. We extended the three component model presented previously to include multiple connections between the tool and holder along the interference contact within the holder. We believe this to be a preferred solution because the stiffness/damping is now located at the appropriate locations, rather than artificially at the junction between the portions of the tool inside and outside the holder. Finite element models are developed in Part 2 to determine the position-dependent stiffness and equivalent viscous damping values for a thermal shrink fit connection between the tool and holder. These values are used to populate the K matrices (Eq. 2) presented here. Experimental results are also provided in Part 2.

REFERENCES

- [Agapiou, 2004] Agapiou, J.; "A Methodology to Measure Joint Stiffness Parameters for Toolholder/spindle Interfaces"; *Transactions of NAMRI/SME*, Vol. 32, pp. 503-510; 2004
- [Bishop et al., 1960] Bishop, R.E.D.; Johnson, D.C.; The Mechanics of Vibration, Cambridge University Press, Cambridge; 1960
- [Burns et al., 2005] Burns, T.; Schmitz, T.; "A Study of Linear Joint and Tool Models in Spindle-Holder-Tool Receptance Coupling"; In: *Proceedings of 2005 American Society of Mechanical Engineers International Design Engineering Technical*

- Conferences and Computers and Information in Engineering Conference*, DETC2005-85275, Long Beach, CA; 2005
- [Cheng et al., 2005] Burns, T.; Schmitz, T.; "An Approach for Micro End mill Frequency Response Predictions"; In: *Proceedings of American Society of Mechanical Engineers International Mechanical Engineering Congress and Exposition*, IMECE2005-81215, Orlando, FL; 2005
- [Kivanc et al., 2004] Kivanc, E.B.; Budak, E.; "Structural Modeling of End Mills for Form Error and Stability Analysis"; *International Journal of Machine Tools and Manufacture*, Vol. 44(11), pp. 1151-1161; 2004
- [Park et al., 2003] Park, S.; Altintas, Y.; Movahhedy, M.; "Receptance Coupling for End Mills"; *International Journal of Machine Tools and Manufacture*, Vol. 44(11), pp. 1151-1161; 2003
- [Schmitz et al., 2003] Schmitz, T.; Burns, T.; "Receptance Coupling for High-Speed Machining Dynamics Prediction"; In: *Proceedings of the 21st International Modal Analysis Conference*, February 3-6, Kissimmee, FL; 2003
- [Schmitz et al., 2001a] Schmitz, T.; Davies, M.; Kennedy, M.; "Tool Point Frequency Response Prediction for High-Speed Machining by RCSA"; *Journal of Manufacturing Science and Engineering*, Vol. 123, pp. 700-707; 2001
- [Schmitz et al., 2001b] Schmitz, T.; Davies, M.; Medicus, K.; Snyder, J.; "Improving High-Speed Machining Material Removal Rates by Rapid Dynamic Analysis"; *Annals of the CIRP*, Vol. 50(1), pp. 263-268; 2001
- [Schmitz et al., 2000] Schmitz, T.; Donaldson, R.; "Predicting High-Speed Machining Dynamics by Substructure Analysis"; *Annals of the CIRP*, Vol. 49(1), pp. 303-308; 2000
- [Schmitz et al., 2005a] Schmitz, T.; Duncan, G.S.; "Three-Component Receptance Coupling Substructure Analysis for Tool Point Dynamics Prediction"; *Journal of Manufacturing Science and Engineering*, Vol. 127(4), pp. 781-790; 2005
- [Schmitz et al., 2006] Schmitz, T.; Duncan, G.S.; "Receptance Coupling for Dynamics Prediction of Assemblies with Coincident Neutral Axes"; *Journal of Sound and Vibration*, Vol. 289(4-5), pp. 1045-1065; 2006
- [Schmitz et al., 2005b] Schmitz, T.; Duncan, G.S.; Zahner, C.; Dyer, J.; Tummond, M.; "Improved Milling Capabilities through Dynamics Prediction: Three Component Spindle-Holder-Tool Model"; In: *Proceedings of 2005 National Science Foundation DMII Grantees Conference*, Scottsdale, AZ; 2005
- [Yigit et al., 2002] Yigit, A.S.; Ulsoy, A.G.; "Dynamic Stiffness Evaluation for Reconfigurable Machine Tools including Weakly Non-linear Joint Characteristics"; *Proceedings of the I MECH E Part B Journal of Engineering Manufacture*, Vol. 216(1), pp. 87-101; 2002
- [Zhang et al., 2003] Zhang, G.P.; Huang, Y.M.; Shi, W.H.; Fu, W.P.; "Predicting Dynamic Behaviors of a Whole Machine Tool Structure Based on Computer-aided Engineering"; *International Journal of Machine Tools and Manufacture*, Vol. 43, pp. 699-706; 2003